ChemComm

COMMUNICATION

View Article Online
View Journal

Cite this: DOI: 10.1039/c5cc07989f

Received 23rd September 2015,
Accepted 15th October 2015

DOI: 10.1039/c5cc07989f

www.rsc.org/chemcomm

Near-IR mediated intracellular uncaging of NO from cell targeted hollow gold nanoparticles†

Elizabeth S. Levy,‡ Demosthenes P. Morales,‡ John V. Garcia, Norbert O. Reich* and Peter C. Ford*

We demonstrate modulation of nitric oxide release in solution and in human prostate cancer cells from a thiol functionalized cupferron (TCF) absorbed on hollow gold nanoshells (HGNs) using near-infrared (NIR) light. NO release from the TCF–HGN conjugates occurs through localized surface heating due to NIR excitation of the surface plasmon. Specific HGN targeting is achieved through cell surface directed peptides, and excitation with tissue penetrating NIR light provides unprecedented spatio-temporal control of NO delivery to biological targets.

Nitric oxide (NO) is a bioregulatory small molecule that mediates a diverse range of activities from blood pressure to cell apoptosis depending on its intracellular concentration.[1] There are many potential therapeutic applications of NO delivery; however, this presents a technical challenge owing to NO's diverse and concentration dependent biological responses and associated chemical reactions. For example, low NO concentrations promote cell survival and even proliferation, while higher concentrations result in opposite responses.[2,3] Thus, it is imperative to exercise precise control over the dosage delivered to cellular sites in order to elicit the desired effects and avoid undesirable ones.

One approach is to use light to trigger NO release ("uncaging") from an otherwise inactive precursor, thus allowing precise control of the timing and location of this event. There are now numerous examples of NO uncaging using donor molecules photoactivated by UV-to-visible light;[4–7] however, strong absorptions of cellular components, especially DNA and hemes, interfere with application of these shorter wavelengths.[8] Given that near-infrared light penetrates more deeply and is relatively benign to tissue, these laboratories[9,10] and others[11,12] have been interested in designing systems that employ NIR wavelengths to trigger the photochemical uncaging of various bioactive small molecules. In the present study, we describe a somewhat different tack, namely the use of NIR excitation to trigger the thermochemical release of NO from a thiol functionalized derivative of cupferron, (ammonium *N*-nitroso(4-mercaptomethylphenyl)hydroxylamine, TCF).

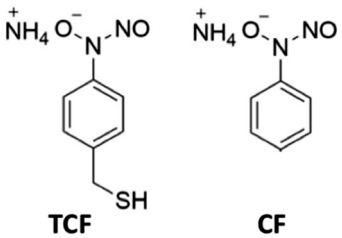

Cupferron (CF) was developed over a century ago as an organic precipitant for copper(II) and iron(III) ions.[13,14] More recently, several workers have studied cupferron derivatives as precursors that are triggered by electrochemical or photochemical oxidation reactions to release one equivalent of the caged NO.[15–17] Notably, much earlier thermal stability studies have shown that simply heating CF leads to decomposition resulting in the release of one equivalent of NO, although the other products of this redox reaction were not identified.[13] The question is: how does one trigger this NO release in a controlled fashion? Our premise is that the rapid heating of hollow gold nanoshells (HGNs) upon excitation of the surface plasmon with NIR light[18–21] will trigger thermochemical NO release from TCF absorbed on the surface (Scheme 1). Described are the preparation of such conjugates and photoexcitation studies that validate this strategy for NO uncaging. Furthermore, we show that orthogonal assembly with a targeting peptide[22] provides the means to direct these nanoparticles to a subset of cells with high precision and efficient uptake. NIR photolysis thus leads to NO delivery with unprecedented spatio-temporal control.

Preparation of TCF–HGN conjugates. The hollow gold nanoshells (~65 nm diameters, ESI,† Fig. S-1)[19,20] and the thiolated cupferron TCF[15,16] were synthesized by published methods as described in the ESI.† The optical spectrum of the HGNs displayed a broad, strong absorption band at λ_{max} ~ 750 nm with an extinction coefficient of $\sim 3 \times 10^{10}$ M^{-1} cm^{-1} (Fig. 1). This band has been attributed to the plasmonic transition of these

Department of Chemistry and Biochemistry, University of California, Santa Barbara, CA, 93106-9510 USA. E-mail: reich@chem.ucsb.edu, ford@chem.ucsb.edu

† Electronic supplementary information (ESI) available: Detailed descriptions of experimental procedures and ten figures. See DOI: 10.1039/c5cc07989f

‡ These authors contributed equally.

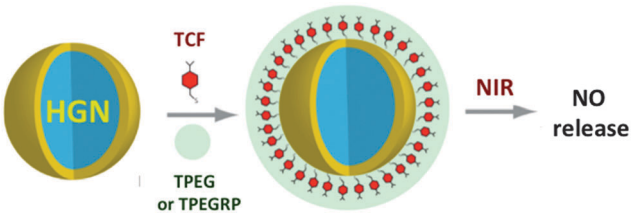

Scheme 1 The surfaces of the hollow gold nanoshells are coated by co-absorption of the thiolated cupferron TCF and of a thiolated PEG (TPEG or TPEGRP), which serves as a protective layer and to enhance aqueous solubility and in the case of TPEGRP provides the cell-targeting peptide. Upon 800 nm laser excitation of the TCF–HGN–TPEG or TCF–HGN–TPEGRP conjugates, HGN surface temperatures are rapidly elevated and NO is released.

metallic nanoparticles.[18,19] Formation of the conjugates between the HGNs and the cupferron derivative TCF takes advantage of the tendency of thiols to form self-assembled monolayers on gold surfaces.[23] In order to prevent nanoparticle aggregation and improve aqueous solubility, this self-assembly was carried out with an equimolar mixture of TCF and a thiolated polyethylene glycol (TPEG, 5 kDa, purchased from Nanocs). A 100 μL volume of solution of TCF and TPEG (both 100 μM) in pH 7.4 PBS with 0.01% Tween20 surfactant was mixed with a 1.0 mL volume of HGNs in 500 μM citrate buffer pH 5.5 (50 pM HGN concentration). The resulting TCF–HGN–TPEG conjugates were washed repeatedly by centrifugation for 10 minutes, decanting the solution from the solid, and then re-suspending in the PBS-Tween20 solution. This procedure was repeated a minimum of 3 times to remove unbound TCF and TPEG. The visible/NIR spectrum of the resulting conjugates (ESI,† Fig. S-2) is qualitatively the same as that found for the HGN particles before modifying the surfaces. As described below and in the ESI,† conjugates with a thiolated polyethylene glycol modified to include the terminally bound targeting peptide RPARPAR (TCF–HGN–TPEGRP) and conjugates that do not present the TCF (HGN–TPEG or HGN–TPEGRP) were prepared by analogous procedures.

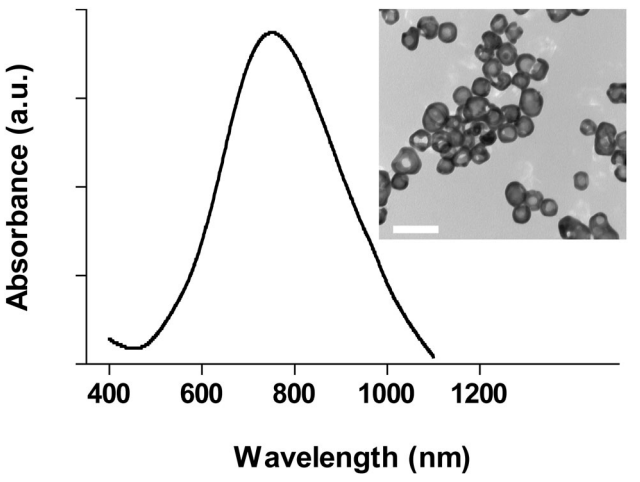

Fig. 1 Characteristic NIR absorption spectrum of the hollow gold nanoshells used to prepare the TCF–HGN–TPEG conjugates. The band centered at ~750 nm is attributed to surface plasmonic excitation. Inset: TEM of these HGNs. Scale bar is 100 nm.

The loading of the thiolated cupferron on the HGN conjugates was evaluated by heating a 100 μL volume of the nanoparticle suspension at 80 °C for 8 h in a closed vessel having a port fitted with a syringe cap. A gas-tight syringe was then used to withdraw a sample of the gaseous headspace and transfer this to a GE Siever's nitric oxide analyzer (NOA). The amount of NO thus detected by the NOA indicated that 300 pmol of NO were released from the solution containing the TCF–HGN–TPEG conjugate. Further heating did not result in the release of additional NO, so it was concluded that all the TCF had undergone thermal decomposition. The HGN concentration in the 100 μL solution was calculated to be 48 pM from the optical density. Thus, by drawing on the earlier observation that one mole of NO is generated thermally for each mole of cupferron present,[13] one can calculate the surface loading to be $\sim 6 \times 10^4$ TCF molecules per nanoparticle (Fig. 2, right).

As a control, a nanoparticle suspension was prepared from the HGNs by adding equimolar amounts of TPEG and the non-thiolated cupferron CF. These were isolated and cleaned in a similar manner, and then re-suspended in pH 7.4 PBS-Tween20 solution. Analogous heating at 80 °C for 8 h and sampling of the headspace showed that the NO released was only 10% that released by the TCF–HGN–TPEG conjugates. The observation that some NO is released by the control suggests that the preparation of HGN–TPEG ensemble in the presence of CF retains some of that cupferron, perhaps trapped in the organic surface coating. However, the much stronger association of TCF in the TCF–HGN–TPEG conjugates is clearly evident.

At physiological temperatures, both cupferron and thiolated cupferron proved to be quite stable. This was tested by maintaining the temperature of a 100 μM sample of each in pH 7.4 PBS-Tween20 solution for a period of 13 h at 37 °C in a closed vessel. The headspace was then sampled and analyzed, but NO release was not observed in either case. (The NOA detection limit is ~0.5–1 picomoles). Furthermore, TCF displays very little toxicity as tested with the human prostate cell line, PPC-1.

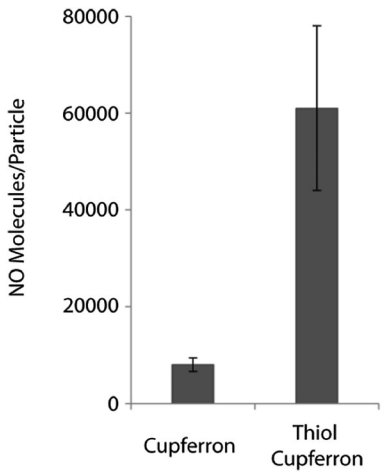

Fig. 2 Right: Nitric oxide release after heating a suspension of the washed and isolated TCF–HGN–TPEG conjugates for 8 h at 80 °C. Left: NO release from comparable solution of conjugates prepared with CF rather than with TCF. The much stronger signal for TCF (right) can be attributed to the self-assembly of TCF on the HGN.

Cells incubated for 24 h with increasing TCF concentrations showed little effect on cell viability up to 10 μM in the medium according to the PrestoBlue staining assay (Life Technologies). Higher concentrations did show some modest toxicity (ESI,† Fig. S-3).

Excitation of TCF–HGN conjugates. NIR irradiation at a wavelength corresponding to excitation of the surface plasmon of the thiolated cupferron-hollow gold nanoparticle conjugates leads to NO release. A solution of the TCF–HGN–TPEG conjugates (48 pM in 100 μL volume of the pH 7.4 PBS-Tween20 solution) in a sealed quartz cuvette was subjected to 800 nm excitation by the high intensity pulses from a Ti:sapphire ultrafast pulsed laser. The result was controlled NO release. Irradiation for 30 s at 1 kHz (140 fs pulses, 5 mm beam diameter, Gaussian profile pulses) at an average power of 5 W cm^{-2} generated 240 pmol of NO as detected by sampling the gaseous headspace and measuring the NO content using the NOA. This quantity corresponds to 80% conversion of the total TCF present, according to the above data on the loading. Similarly, 800 nm photolysis with the same laser system but at the lower average laser powers 0.9, 1.5 and 2.4 W cm^{-2} generated 42, 126 and 156 pmol of NO, respectively, from analogous solutions of the TCF–HGN–TPEG conjugates (Fig. 3).

As previously reported,[23] the high peak intensities of the pulsed ultrafast laser system are exceptionally effective in the rapid heating of gold nanoparticles with NIR light. However, it is notable that NO release could also be effected by excitation with a continuous wave (CW) NIR laser operating at 800 nm, although the process was considerably less efficient. In that case, it was necessary to focus the CW beam to a diameter of 0.9 mm where the intensity was 157 W cm^{-2}. Irradiation of a comparable solution of the TCF–HGN–TPEG conjugates at this intensity for 60 s gave 41 pmol NO, while irradiation at 78.5 W cm^{-2} gave 9.4 pmol NO (ESI,† Fig. S-5). This behavior is consistent with non-linear absorption of light by the HGN surface plasmon leading to localized heating and consequently to thermochemical NO release from the TCF. Notably, there were only modest changes in the bulk solution temperatures with excitation from either the pulsed or continuous laser (ESI,† Fig. S-6).

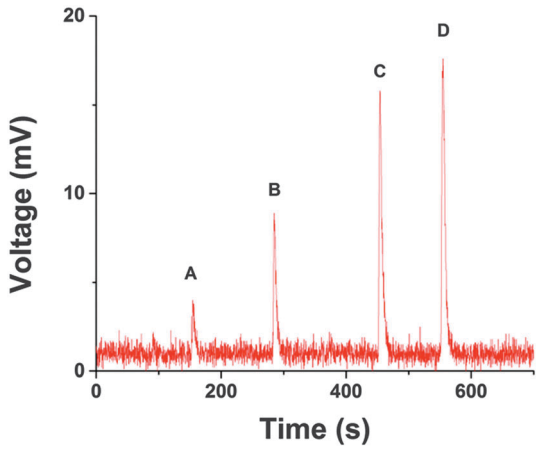

Fig. 3 NOA signal demonstrating the release of NO from TCF–HGN–TPEG conjugates upon excitation with a 800 nm pulsed laser operating at 1 KHz. Signals are for different excitation powers 0.9 W cm^{-2} (A) 1.5 W cm^{-2} (B), 2.4 W cm^{-2} (C) and 5 W cm^{-2} (D). (NOA signal: 1 mV = ~13.3 pmol). Signal D corresponds to release of ~80% of the NO available based on the TCF loading of the TCF–HGN–TPEG conjugates (see ESI,† Fig. S-4).

Targeting with peptides. Cellular internalization of the nanoparticles was facilitated by Neuropilin-1 receptor mediated endocytosis through coupling the C-end Rule (CendR) peptide, RPARPAR,[24] to the end of a 5 kDa thiolated polyethylene glycol (see ESI†). This peptide derivatized thiolated PEG (TPEGRP) was then used to prepare TCF–HGN–TPEGRP conjugates in the manner used to prepare the TCF–HGN–TPEG analogs. Quantification of the peptide was done by comparison of rhodamine dye label on the sequence against a standard calibration curve. This gave the estimate of ~3000 peptide per particle after KCN etching (data not shown). Microscopy analysis of HGN internalization confirms that nanoparticles are readily internalized within 2 h only for cells that overexpress the Neuropilin-1 receptor, such as PPC-1 prostate cells. The HeLa cell line, lacking Neuropilin-1 receptor did not do so (ESI,† Fig. S-7 and S-8).

The release of NO from the TCF–HGN–TPEGRP conjugates inside the cells was tested by using the diaminofluorescein diacetate fluorescent reporter (DAF-2 DA). A control analog without TCF was generated by omitting the addition of TCF (HGN–TPEGRP). Both HGN–TPEGRP and TCF–HGN–TPEGRP readily underwent endocytosis with two different prostate cancer cell lines as seen in the microscopy images shown in ESI,† Fig. S-7 and S-8 for the PPC-1 cells and in Fig. 4 for the 22Rv1 cells, which are also positive for Neuropilin-1 overexpression.[25] Since background fluorescence problems made it difficult to detect NO production in the PPC-1 cells, those experiments were conducted using the 22Rv1 cells.

As described in the ESI,† the 22Rv1 cells were first treated with the nitric oxide synthase inhibitor, L-N^G-nitroarginine methyl ester

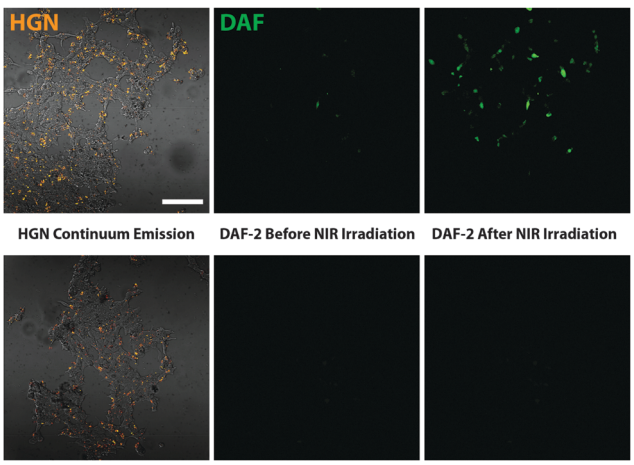

Fig. 4 Cell-specific targeting of NO release with NIR-mediated spatio-temporal control. The 22Rv1 cells were treated with TCF–HGN–TPEGRP conjugates and the NO was detected using DAF-2 DA fluorescent reporter. First column: incorporation of HGN is visualized by continuum emission (orange) localized within cells during irradiation. Scale bar is 100 μm. Top row: 22Rv1 cells treated with TCF–HGN–TPEGRP exhibit increased fluorescence from the reporter (green) upon laser irradiation with 800 nm pulsed laser light indicating generation of NO. Bottom row: Cells treated with HGN–TPEGRP do not increase in fluorescence indicating that NO was not generated. (See also ESI,† Fig. S-9.)

(L-NAME). One set of cells was then incubated with the TCF–HGN–TPEGRP conjugates for 2 h, while a second set was incubated with the HGN–TPEGRP analog without the caged NO TCF, and repeatedly washed with buffer to remove non-internalized nanoparticles before use. Both sets of cells were incubated with DAF-2 DA (see ESI†). Imaging was accomplished using a laser scanning confocal two-photon microscope (Olympus Fluoview 1000 MPE) equipped with a tunable fs pulsed laser, as well as a 473 nm CW laser. The continuum emission of the hollow gold nanoshells resulting from 800 nm excitation demonstrates nanoparticle internalization for both experiments. Fig. 4 (left panels) shows the gold particles within the outlines of the cells. Before NIR excitation, virtually no fluorescence was seen from either set of cells when probed using single photon continuous irradiation at 473 nm (Fig. 4, center panels). However, upon excitation at 800 nm by rastering the fs pulsed laser 5× through the two sets of cells, the 22Rv1 cells treated with the TCF–HGN–TPEGRP conjugates clearly showed fluorescence, indicating NO generation as detected by the fluorophore formation with the DAF-2 DA (Fig. 4, top right). In contrast, cells treated similarly with the HGN–TPEGRP conjugate (without the NO donor) did not exhibit any change in fluorescence before or after irradiation with 800 nm pulsed laser light (Fig. 4, bottom right).

Notably, irradiation of the TCF–HGN–TPEGRP conjugates internalized in cells showed little alteration in cellular viability at 2.4 W cm^{-2} excitation power but modest decreases (20–40%) in viability at 5 W cm^{-2} (ESI,† Fig. S-10).

In summary, we have demonstrated that using NIR light to excite the surface plasmon of hollow gold nanoshells is a viable strategy for the controlled release of NO in solution and in human prostate cancer cells. While others have described gold nanoparticle platforms for NO delivery,[26–28] the present report is the first to utilize NIR light with such systems. This NO uncaging can be attributed to rapid heating of the thiolated cupferron bound to the HGN surfaces of the TCF–HGN–TPEG conjugates upon NIR irradiation with a pulsed laser at frequencies resonant with the surface plasmon. The quantities of NO released in the small solution volumes irradiated (Fig. 3) correspond to ''instantaneous'' NO concentrations ranging from 420 nM to 2.4 μM. Further studies are required to improve the nanoparticle capabilities for releasing NO; however, given that nitric oxide bioactivity is evident even at nanomolar concentrations,[2,3] it is clear that this technique generates biologically relevant NO concentrations within the irradiated volumes. The power dependence for photoexcitation of the nanoshell platform will allow for tuning the intracellular concentrations delivered. The combination of the cell-specific targeting peptide in the TCF–HGN–TPEGRP conjugates and NIR-mediated control of NO release provides an unprecedented basis for investigating the spatio-temporal response to this important bio-regulatory small molecule.

None of the authors have a financial conflict of interest to declare.

This work was supported by NSF Chemistry Division grants (CHE-1058794 and CHE-1405062) to PCF, a National Institutes of Health grant (R01 EB012637) to NOR and by a fellowship to ESL from the UCSB IRES-ECCI Program (NSF grant OISE-1065581). Two photon microscopy was available through NIH (1 S10 OD010610-01A1) and the NRI-MCDB Microscopy Facility. We thank E. Ruoslahti for cell lines. We thank A. Mikailovsky for his help with the ultrafast laser experiments, M. Raven for discussions pertaining to the two photon microscope and A. E. Pierri for many helpful discussions.

References

1 L. J. Ignarro, *Nitric Oxide: Biology and Pathobiology*, Elsevier Inc., Burlington, MA, 2nd edn 2010.
2 S. Mocellin, V. Bronte and D. Nitti, *Med. Res. Rev.*, 2007, **27**, 317–352.
3 D. D. Thomas, L. A. Ridnour, J. S. Isenberg, W. Flores-Santana, C. H. Switzer, S. Donzelli, P. Hussain, C. Vecoli, N. Paolocci, S. Ambs, C. A. Colton, C. C. Harris, D. D. Roberts and D. A. Wink, *Free Radical Biol. Med.*, 2008, **45**, 18–31.
4 P. C. Ford, J. Bourassa, K. M. Miranda, B. Lee, I. Lorkovic, S. Boggs, S. Kudo and L. Laverman, *Coord. Chem. Rev.*, 1998, **171**, 185–202.
5 U. Schatzschneider, *Eur. J. Inorg. Chem.*, 2010, 1451–1467.
6 B. Heilman and P. K. Mascharak, *Philos. Trans. R. Soc., A*, 2013, **371**(1995), 20120368.
7 S. Sortino, *Chem. Soc. Rev.*, 2010, **39**, 2903–2913.
8 A. M. Smith, M. C. Mancini and S. Nie, *Nat. Nanotechnol.*, 2009, **4**, 710–711.
9 J. V. Garcia, F. Zhang and P. C. Ford, *Philos. Trans. R. Soc., A*, 2013, **371**, 20120129.
10 P. C. Ford, *Acc. Chem. Res.*, 2008, **41**, 190–200.
11 (*a*) G. Bort, T. Gallavardin, D. Ogden and P. I. Dalko, *Angew. Chem., Int. Ed.*, 2013, **52**, 4526–4537; (*b*) J. D. Mase, A. O. Razgoniaev, M. K. Tschirhart and A. D. Ostrowski, *Photochem. Photobiol. Sci.*, 2015, **14**, 775–785.
12 (*a*) X. Zhang, G. Tian, W. Yin, L. Wang, X. Zheng, L. Yan, J. Li, H. Su, C. Chen, Z. Gu and Y. Zhao, *Adv. Funct. Mater.*, 2015, **25**, 3049–3056; (*b*) E. Ruggiero, J. Hernandez-Gil, J. C. Mareque-Rivasa and L. Salassa, *Chem. Commun.*, 2014, **51**, 2091.
13 W. Wendlandt, S. I. Ali and C. H. Stembridge, *Analytica Chemica Act*, 1964, **31**, 501–550.
14 O. Baudisch, *Chem.–Ztg.*, 1909, **33**, 1298, as noted in ref. 13.
15 Y. C. Hou, W. H. Xie, A. J. Janczuk and P. G. Wang, *J. Org. Chem.*, 2000, **65**, 4333–4337.
16 Y. C. Hou, Y. Chen, N. Amro, K. Wadu-Mesthrige, P. R. Andreana, P. R. Liu and P. G. Wang, *Chem. Commun.*, 2000, 1831–1832.
17 E. Vittorino, E. Cicciarella and S. Sortino, *Chem. – Eur. J.*, 2009, **15**, 6802–6804.
18 Z. Qin and J. C. Bischof, *Chem. Soc. Rev.*, 2012, **41**, 1191–1217.
19 G. Wu, A. Mikhailovsky, H. A. Khant and J. A. Zasadzinski, *Methods Enzymol.*, 2009, **464**, 279–307.
20 G. Braun, A. Pallaoro, G. Wu, D. Missirlis, J. A. Zasadzinski, M. Tirrell and N. O. Reich, *ACS Nano*, 2009, **3**, 2007–2015.
21 P. K. Jain, W. Qian and M. A. El-Sayed, *J. Am. Chem. Soc.*, 2006, **128**, 2426–2433.
22 K. N. Sugahara, T. Teesalu, P. P. Karmali, V. R. Kotamraju, L. Agemy, O. M. Girard, D. Hanahan, R. F. Mattrey and E. Ruoslahti, *Cancer Cell*, 2009, **16**, 510–520.
23 (*a*) C. Vericat, M. E. Vela, G. Benitez, P. Carro and R. C. Salvarezza, *Chem. Soc. Rev.*, 2010, **39**, 1805–1834; (*b*) X. Huang, A. Pallaoro, G. B. Braun, D. P. Morales, M. O. Ogunyankin, J. Zasadzinski and N. O. Reich, *Nano Lett.*, 2014, **14**, 2046–2051; (*c*) D. P. Morales, G. B. Braun, A. Pallaoro, R. Chen, X. Huang, J. A. Zasadzinski and N. O. Reich, *Mol. Pharmaceutics*, 2015, **12**, 600–609.
24 T. Teesalu, K. N. Sugahara, V. R. Kotamraju and E. Ruoslahti, *Proc. Natl. Acad. Sci. U. S. A.*, 2009, **106**, 16157.
25 K. N. Sugahara, T. Teesalu, P. P. Karmali, V. R. Kotamraju, L. Agemy, O. M. Girard, D. Hanahan, R. F. Mattrey and E. Ruoslahti, *Cancer Cell*, 2009, **16**, 510–520.
26 N. Nakatsubo, H. Kojima, K. Kikuchi, H. Nagoshi, Y. Hirata, D. Maeda, Y. Imai, T. Irimura and T. Nagano, *FEBS Lett.*, 1998, **427**, 263.
27 H. T. T. Duong, N. N. M. Adnan, N. Barraud, J. S. Basuki, S. K. Kutty, K. Jung, N. Kumar, T. P. Davis and C. Boyer, *J. Mater. Chem. B*, 2014, **2**, 5003–5011.
28 P. Taladriz-Blanco, P. J. Pérez-Juste, N. Kandoth, P. Hervés and S. Sortino, *J. Colloid Interface Sci.*, 2013, **407**, 524–528.